

Diagnostics of Rotor Damages of Three-Phase Induction Motors Using Acoustic Signals and SMOFS-20-EXPANDED

Adam GLOWACZ

AGH University of Science and Technology
al. A. Mickiewicza 30, 30-059 Kraków, Poland; e-mail: adglow@agh.edu.pl

(received October 16, 2015; accepted April 15, 2016)

A fault diagnostics system of three-phase induction motors was implemented. The implemented system was based on acoustic signals of three-phase induction motors. A feature extraction step was performed using SMOFS-20-EXPANDED (shortened method of frequencies selection-20-Expanded). A classification step was performed using 3 classifiers: LDA (Linear Discriminant Analysis), NBC (Naive Bayes Classifier), CT (Classification Tree). An analysis was carried out for incipient states of three-phase induction motors measured under laboratory conditions. The author measured and analysed the following states of motors: healthy motor, motor with one faulty rotor bar, motor with two faulty rotor bars, motor with faulty ring of squirrel-cage. Measured and analysed states were caused by natural degradation of parts of the machine. The efficiency of recognition of the analysed states was good. The proposed method of fault diagnostics can find application in protection of three-phase induction motors.

Keywords: induction motor; machine; acoustic signal; acoustic emission; fault diagnostics.

1. Introduction

Diagnostics of machines is a very interesting topic of research (ATTOUI, OMEIRI, 2015; BEDKOWSKI, BARANSKI, 2014; GLOWACZ, 2015; HEMMATI *et al.*, 2016; HWANG *et al.*, 2015; IRFAN *et al.*, 2015; JENA, PANIGRAHI, 2015; JIANG *et al.*, 2016; KLUSKA-NAWARECKA *et al.*, 2014; KROLCZYK *et al.*, 2016a; 2016b; LI *et al.*, 2016; SAPENA-BANO *et al.*, 2015; VAN HECKE *et al.*, 2016; YOON, HE, 2015; ZHANG *et al.*, 2015). Therefore, fault diagnosis techniques should be developed to prevent sudden stops in the industry. Breakdowns may result in economic losses, so it is important to analyse various faults and machines. Recently some methods based on vibration, acoustic, thermal, and electrical signals were developed to check the mechanical and electrical condition of machines (FIGLUS *et al.*, 2014; GLOWACZ, GLOWACZ, 2007; GLOWACZ, ZDROJEWSKI, 2009; GLOWACZ *et al.*, 2012; GONZALEZ-CORDOBA *et al.*, 2016; JOZWIK, 2016; MIKA, JOZWIK, 2016; KANG *et al.*, 2015; KROLCZYK *et al.*, 2014; LARA *et al.*, 2015; MICHALAK *et al.*, 2013; PERUN, STANIK, 2015; SMALCERZ, 2013; WEGIEL *et al.*, 2007). Some of them had a high efficiency of signal recognition. However, the results were obtained for limited data. This is a motivation to de-

velop better methods of fault diagnosis of induction motors. In this paper the author measured and analysed rotor faults. The analysed rotor faults were as follows: one faulty rotor bar, two faulty rotor bars, faulty ring of squirrel-cage. The author implemented a system of recognition of acoustic signals. This system was based on a microphone and a computer (Fig. 1).

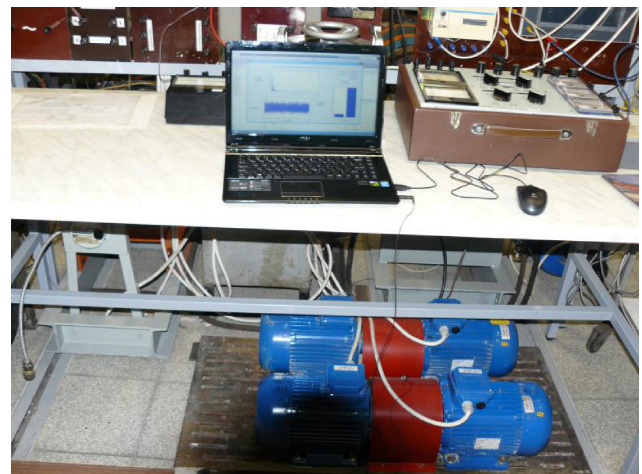


Fig. 1. Analysed three phase induction motors and system of fault diagnostics.

2. Method of recognition of acoustic signal of three phase induction motor

The analysed method of recognition of acoustic signals of three phase induction motor consists of 6 steps of data processing (Fig. 2). Step 1 is recording of signal of three phase induction motor. Various types of condenser microphones and computers can be used for this step (KULKA, 2011). The distance from the microphone to induction motor was essential. The microphone was set at a distance of 0.02 to 0.05 m from the machine. Placement of the microphone will have impact on the outcome of the research. If the microphone is placed 10 meters from the machine, the results of recognition may be different. The results are related to the training set (samples of sounds). Test samples and training samples should be measured at the same distance from the machine. The obtained soundtrack should have sampling frequency 44100 Hz, one channel (mono) and uncompressed audio format. Next, the obtained soundtrack is split into small samples. After that amplitude normalisation is carried out. The FFT algorithm is conducted at step 4 (DUSPARA *et al.*, 2014; STEPIEN, 2014). Calculation of SMOFS-20-EXPANDED is carried out at step 5. The pattern creation process and the identification process are executed at step 6.

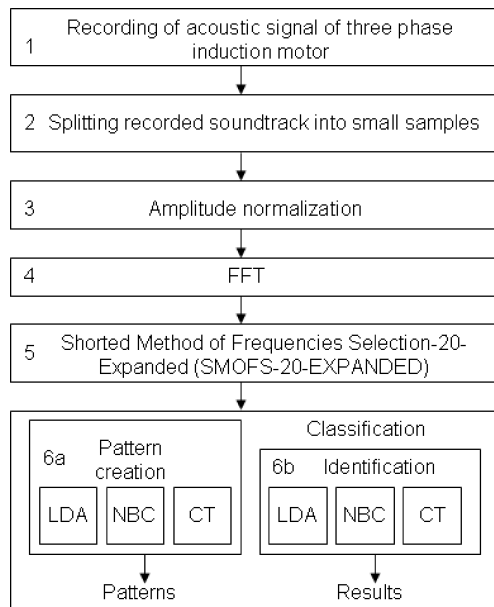


Fig. 2. Analysed method of recognition of acoustic signal of three phase induction motor using FFT, SMOFS-20-EXPANDED, LDA (Linear Discriminant Analysis), NBC (Naive Bayes classifier), CT (classification tree).

2.1. Splitting recorded soundtrack

Splitting recorded soundtrack into small samples was implemented in the presented system. Perl lan-

guage was used for this purpose. The implemented program split signal into samples with various length of time (default 5 seconds).

2.2. Amplitude normalization and FFT

The amplitude normalisation was used to compare acoustic signals of three phase induction motor. The amplitude normalisation divided each point of signal by the maximum value. The obtained normalised signal was in the range $[-1, 1]$. The FFT method used Hamming window with the length of 32768 (1 window = $32768/44100 = 0.743$ seconds). For this reason the FFT spectrum had 16384 values. This number (16384) was sufficient to represent the analysed data.

2.3. Shortened method of frequencies selection-20-EXPANDED

Research from around the world has been developing new complex methods of feature extraction from acoustic signals. Some of them are based on the FFT. One of them is SMOFS-20-EXPANDED (shortened method of frequencies selection-20-Expanded). This method is based on differences between amplitudes of frequencies of analysed acoustic signals. Faulty states of three phase induction motor can generate different spectra of acoustic signals. These spectra are analysed by the proposed method. SMOFS-20-EXPANDED consists of 7 steps:

1. The first step is calculation of the FFT spectrum of the acoustic signal. The following spectra of acoustic signals of induction motor are defined by vectors: $\mathbf{hid} = [hid_1, hid_2, \dots, hid_{16384}]$ – healthy motor, $\mathbf{frb} = [frb_1, frb_2, \dots, frb_{16384}]$ – motor with faulty rotor bar, $\mathbf{frbs} = [frbs_1, frbs_2, \dots, frbs_{16384}]$ – motor with two faulty rotor bars, $\mathbf{frsq} = [frsq_1, frsq_2, \dots, frsq_{16384}]$ – motor with faulty ring of squirrel-cage.
2. The second step is calculation of differences of spectra of acoustic signals: $\mathbf{hid-frb}$, $\mathbf{hid-frbs}$, $\mathbf{hid-frsq}$, $\mathbf{frb-frbs}$, $\mathbf{frb-frsq}$, $\mathbf{frbs-frsq}$.
3. Calculate absolute values of obtained differences: $|\mathbf{hid-frb}|$, $|\mathbf{hid-frbs}|$, $|\mathbf{hid-frsq}|$, $|\mathbf{frb-frbs}|$, $|\mathbf{frb-frsq}|$, $|\mathbf{frbs-frsq}|$.
4. Use the following formula to obtain selected frequencies:

$$||AS_n| - |AS_m|| > TS_x, \quad (1)$$

where TS_x – threshold of selection after x iterations (Formula 1), $||AS_n| - |AS_m||$ – difference between amplitudes of frequencies for states n and m of the analysed motor, AS_n – amplitude of frequency of state n of the analysed motor, AS_m – amplitude of frequency of state m of the analysed motor.

5. TS_x is calculated for x iterations according to the following formulas:

$$TS_x = \frac{\sum_{NAF_x=1}^{NAF_x} ||AS_n| - |AS_m||}{NAF_x}, \quad (2)$$

$$NAF_x \leq 20, \quad (3)$$

NAF_x is a number of amplitudes of frequencies. If the value NAF_x is greater than 20, SMOFS-20-EXPANDED used the following expression (Formula 2). SMOFS-20-EXPANDED stops its calculations if the value NAF_x is smaller or equal to 20. NAF_x is the number of frequencies after x iterations (initially $NAF_1 = 16384$, the FFT calculates 16384 amplitudes of frequencies for the window length 32768, see Subsec. 2.2). SMOFS-20-EXPANDED calculates the feature vector with 1-20 features, $NAF_x \leq 20$). The parameter NAF_x depends on the number of analysed acoustic signals. Sometimes the differences between amplitudes of frequencies of states may have maximum values at different frequencies. It can be a problem.

Let us analyse the following examples. SMOFS-20-EXPANDED selects frequencies 130, 230, 330, 430, 530, 630, 730 Hz for states S1 and S2. SMOFS-20-EXPANDED selects frequencies 130, 230, 330, 440, 540, 600 Hz for states S2 and S3. SMOFS-20-EXPANDED selects frequencies 120, 220, 320, 440, 540 Hz for states S1 and S3. There is no common frequency for states S1, S2, S3. Frequencies 130, 230, 330, 440, 540 Hz are common for two states. In this case frequencies 130, 230, 330, 440, 540 Hz are the best for analysis.

This will happen for 4 or more analysed states of the motor. For this purpose the parameter CF is used.

6. Set the parameter $CF = (\text{number of required common amplitudes of frequencies}) / (\text{number of all selected amplitudes of frequencies})$. This parameter is responsible for common frequencies. For example, the parameter CF is equal 0.64, then 2 of 3 frequencies are required $((2/3) > 0.64)$ to make decision about selection of common frequencies. In the mentioned example 130, 230, 330, 440, 540 Hz are selected for $CF = 0.64$. If the parameter CF is equal 0.67 $((2/3) < 0.67)$, none of the frequencies will be selected. If the parameter CF is equal 0.32 $((1/3) > 0.32)$, all frequencies will be selected. Of course $CF = 0.32$ is not a good value for analysis.

7. Form feature vector based on common frequencies.

The author proposed a block diagram of SMOFS-20-EXPANDED (Fig. 3).

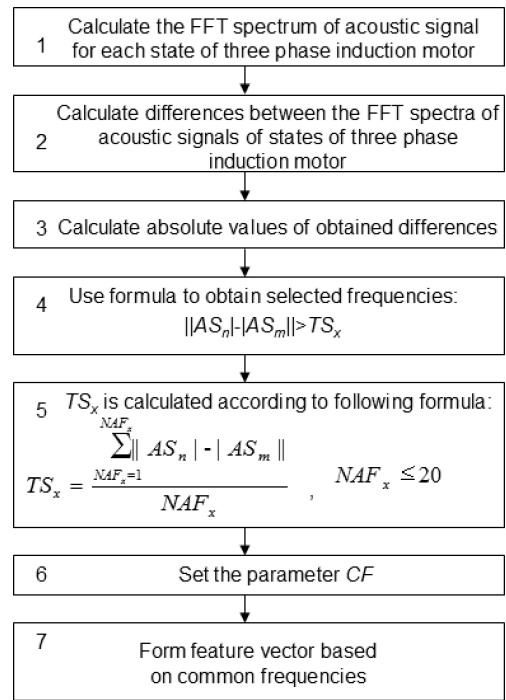


Fig. 3. Block diagram of SMOFS-20-EXPANDED.

The differences between the FFT spectra of the analysed acoustic signals of three phase induction motor are presented (Figs. 4–9).

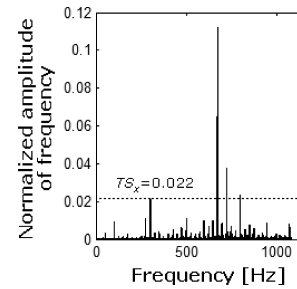


Fig. 4. Difference between the FFT spectra of acoustic signal of healthy state of three phase induction motor and acoustic signal of three phase induction motor with faulty rotor bar (|hid-frb|) and parameter TS_x for SMOFS-20-EXPANDED (selection of 5 frequencies).

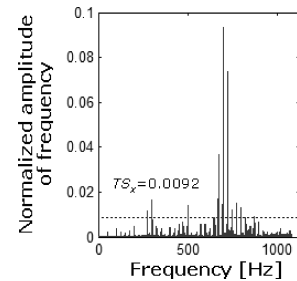


Fig. 5. Difference between the FFT spectra of acoustic signal of healthy state of three phase induction motor and acoustic signal of three phase induction motor with two faulty rotor bars (|hid-frbs|) and parameter TS_x for SMOFS-20-EXPANDED (selection of 19 frequencies).

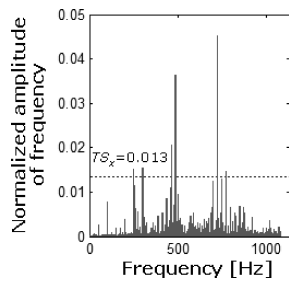


Fig. 6. Difference between the FFT spectra of acoustic signal of healthy state of three phase induction motor and acoustic signal of three phase induction motor with faulty ring of squirrel-cage ($|hid-frsq|$) and parameter TS_x for SMOFS-20-EXPANDED (selection of 9 frequencies).

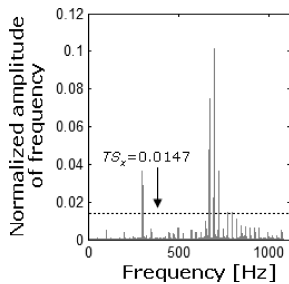


Fig. 7. Difference between the FFT spectra of acoustic signal of three phase induction motor with faulty rotor bar and acoustic signal of three phase induction motor with two faulty rotor bars ($|frb-frbs|$) and parameter TS_x for SMOFS-20-EXPANDED (selection of 10 frequencies).

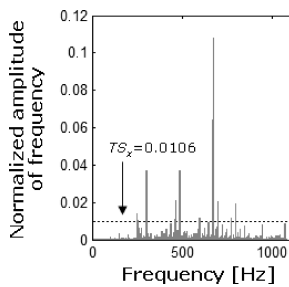


Fig. 8. Difference between the FFT spectra of acoustic signal of three phase induction motor with faulty rotor bar and acoustic signal of three phase induction motor with faulty ring of squirrel-cage ($|frb-frsq|$) and parameter TS_x for SMOFS-20-EXPANDED (selection of 16 frequencies).

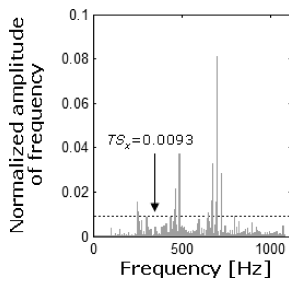


Fig. 9. Difference between the FFT spectra of acoustic signal of three phase induction motor with two faulty rotor bars and acoustic signal of three phase induction motor with faulty ring of squirrel-cage ($|frbs-frsq|$) and parameter TS_x for SMOFS-20-EXPANDED (selection of 17 frequencies).

Five training sets were analysed to select the best frequencies. Each of them had 4 training samples. Selection of common frequencies of 4 states of three-phase induction motor for training set 1 was presented in Table 1.

Table 1. Selection of common frequencies of 4 states of three-phase induction motor for training set 1.

Common Frequencies [Hz]					
hid-frb	hid-frbs	hid-frsq	frb-frbs	frb-frsq	frbs-frsq
300		300	300	300	
301	301		301	301	
		462		462	462
		486		486	486
		487		487	487
670	670		670	670	670
672	672		672	672	672
673			673	673	
	696		696	696	696
	720	720	720		720
721	721	721	721		
723	723	723			
795			795	795	

Table 2. Selection of common frequencies of 4 states of three-phase induction motor depending on the parameter CF and training sets.

$CF = 0.95$ (6 common frequencies)	Frequency [Hz]
Training set 1	–
Training set 2	–
Training set 3	–
Training set 4	–
Training set 5	–
Common frequencies	–
$CF = 0.82$ (5 common frequencies)	Frequency [Hz]
Training set 1	670, 672
Training set 2	696, 697, 721
Training set 3	301, 672, 696
Training set 4	–
Training set 5	672, 721
Common frequencies	–
$CF = 0.64$ (4 common frequencies)	Frequency [Hz]
Training set 1	300, 301, 670, 672, 696, 721
Training set 2	301, 696, 697, 721
Training set 3	301, 672, 696, 721, 797
Training set 4	696, 697, 720, 721, 797
Training set 5	275, 276, 672, 696, 697, 721, 797
Common frequencies	696, 721

For recognition of 4 states of a motor, we need 2 frequencies at least (Table 1 – there is no common frequency). Selection of common frequencies of 4 states of three-phase induction motor depending on the parameter CF and training sets was presented in Table 2.

Amplitudes of frequencies 696, 721 Hz ($\mathbf{hid} = [hid_{517}, hid_{536}]$, $\mathbf{frb} = [frb_{517}, frb_{536}]$, $\mathbf{frbs} = [frbs_{517}, frbs_{536}]$, $\mathbf{frsq} = [frsq_{517}, frsq_{536}]$) formed feature vectors for $CF = 0.64$. Next, the feature vectors were classified by LDA, NBC, CT.

2.4. Classification

Special methods were developed to classify feature vectors. They were called classifiers. In the literature many various classifiers are described (GORNY *et al.*, 2015; HACHAJ, 2012; IZADBAKSH *et al.*, 2015; JUN, KOCHAN, 2014; KANTOCH *et al.*, 2014; KOZIELSKI *et al.*, 2016; MA, CHEN, 2015; ROJ, CICHY, 2015; VALIS, PIETRUCHA-URBANIK; 2014; VETRICHELVAN *et al.*, 2015). Some of them are used for linearly separable patterns, for example, Linear Discriminant Analysis or Support Vector Machine (JAWOREK-KORJAKOWSKA, KLECZEK, 2016; YAGAMI *et al.*, 2015). Other classifiers such as: Nearest Neighbor (MARZEC *et al.*, 2015; STOLINSKI, ZIOLKO, 2015), Gaussian Mixture Model (HACHAJ *et al.*, 2015; PRIBIL, PRIBILOVA, 2014), Naive Bayes classifier, neural networks (DUDEK-DYDUCH *et al.*, 2009; JUN *et al.*, 2016; KALAFAT, SAUSE, 2015; MA, CHEN, 2015; PANEK *et al.*, 2015; ZHANG *et al.*, 2015), classification tree are used for linearly and non-linearly separable patterns.

2.5. Linear Discriminant Analysis

Linear Discriminant Analysis (LDA) was used to classify the feature vectors. This method is based on training and test sets. There was a training set of P -dimensional samples $x_1, x_2, x_3, \dots, x_N$. These samples belonged to classes w_1, w_2, \dots, w_i . Next, a scalar y was obtained by projecting these samples x onto line $y = w^T x$. Next, the method selected one line that maximises the separability of the scalars y . After that LDA calculated the mean vector of each class in x -space and y -space:

$$\begin{aligned} u_i &= \frac{1}{N} \sum_{x \in w_i} x, \\ \tilde{u}_i &= \frac{1}{N} \sum_{y \in w_i} y = w^T u_i. \end{aligned} \quad (4)$$

LDA maximised the difference between the means, normalised by a measure of the within-class scatter. The scatter was expressed by the following formula (5):

$$\tilde{s}_i^2 = \sum_{y \in w_i} (y - \tilde{u}_i)^2. \quad (5)$$

The within-class scatter was expressed by following formula (6):

$$\tilde{s}_1^2 + \tilde{s}_2^2. \quad (6)$$

LDA was defined as a linear function $w^T x$, that maximised the criterion function $J(w)$ defined as (7):

$$J(w) = \frac{|\tilde{u}_1 - \tilde{u}_2|}{\tilde{s}_1^2 + \tilde{s}_2^2}. \quad (7)$$

After performance of the pattern creation process test samples were identified depending on their positions with respect to the calculated hyperplane. More information about LDA can be found in the literature (SHARMA, PALIWAL, 2015).

2.6. Naive Bayes classifier

Naive Bayes classifier can often perform better and faster than other classification methods. This classifier was used for high-dimensional feature vectors. It was based on statistical parameters such as posterior and prior probabilities. The posterior probability was expressed by the following formula:

$$p(x_i|y) = \frac{p(y|x_i)p(x_i)}{p(y)}, \quad (8)$$

where $p(x_i|y)$ is the probability of instance y being in class x_i (posterior probability); $p(y|x_i)$ is the probability of generating instance y given class x_i ; $p(x_i)$ is the probability of occurrence of class x_i ; $p(y)$ is the probability of instance y occurring.

Naive Bayes classifier used training and test sets. The training set was used for training step to estimate a probability distribution. The test set was used for classification step to classify test samples. Test samples were classified depending on the posterior probability (KARANDIKAR *et al.*, 2015; GLOWACZ, GLOWACZ, 2015).

2.7. Classification tree

Classification tree (CT) predicted the output data based on input data (feature vectors). The classifier used root node and leaf nodes to predict the output data. The last leaf nodes contained the output data. The result of classification tree was “true” or “false”. Classification tree performed the following steps:

- Start with all input feature vectors and examine all possible binary splits.
- Select a split with the best optimisation criterion.
- Repeat for the two obtained nodes.
- Stop splitting when a node contains only observations of one class.

More information about classification tree (CT) can be found in the literature (WICKRAMARACHCHI *et al.*, 2016).

3. Analysis of acoustic signals of three-phase induction motor

Four identical induction motors were analysed. The parameters of the motors were the following: $U_{NSV} = 220/380$ V (Δ/Y), $I_{NSC} = 2.52/1.47$ A (Δ/Y), $P_{Motor} = 0.55$ kW, $n_{RS} = 1400$ rpm, where U_{NSV} is the nominal stator voltage, I_{NSC} is the nominal stator current, P_{Motor} is the motor power, n_{RS} is the rotor speed. The motor operated under open loop control.

The analysis was carried out for incipient states of three-phase induction motors measured under laboratory conditions. The author measured and analysed the following states of motors: healthy motor, motor with one faulty rotor bar (Fig. 10), motor with two faulty rotor bars, motor with faulty ring of squirrel-cage (Fig. 11). Measured and analysed states were caused by natural degradation of parts of the motors.

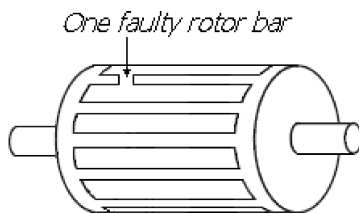


Fig. 10. Rotor of three-phase induction motor with one faulty rotor bar.

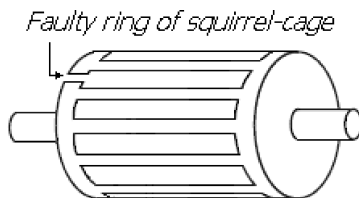


Fig. 11. Rotor of three-phase induction motor with faulty ring of squirrel-cage.

In the pattern creation process 40 five-second training samples were analysed. Patterns were calculated (amplitudes of frequencies 696, 721 Hz). Next, in the identification process 60 test samples were analysed (15 samples for each state of the motor). These 60 test samples were used to evaluate efficiency of recognition of the proposed techniques. The efficiency of recognition was expressed by the following formula:

$$ER = \frac{NPRTS}{NATS} 100\%, \quad (9)$$

where ER is the efficiency of recognition of acoustic signal, $NPRTS$ is the number of the recognised test samples, $NATS$ is the number of test samples in the test set.

The total efficiency of recognition of acoustic signal (TER) was expressed by the formula (10):

$$TER = \frac{ER_H + ER_{FRB} + ER_{FRBS} + ER_{FRSC}}{4}, \quad (10)$$

where TER is the total efficiency of recognition of acoustic signal, ER_H is the efficiency of recognition of acoustic signal of a healthy motor, ER_{FRB} is the efficiency of recognition of acoustic signal of a motor with one faulty rotor bar, ER_{FRBS} is the efficiency of recognition of acoustic signal of a motor with two faulty rotor bars, ER_{FRSC} is the efficiency of recognition of acoustic signal of a motor with a faulty ring of squirrel-cage.

The analysis of recognition of acoustic signals of three-phase induction motors was carried out. The obtained results of recognition are shown in Tables 3–5.

The analysed efficiency of recognition of acoustic signal (ER) was in the range of 53.33–100% for $CF = 0.64$ (Table 3). The total efficiency of recognition of acoustic signal (TER) was equal 76.65% for SMOFS-20-EXPANDED and Linear Discriminant Analysis.

Table 3. Results of recognition of acoustic signal of three phase induction motor using SMOFS-20-EXPANDED and LDA.

State of three-phase induction motor	$CF = 0.64$
	ER [%]
Healthy three-phase induction motor	53.33
Three-phase induction motor with one faulty rotor bar	100
Three-phase induction motor with two faulty rotor bars	100
Three-phase induction motor with faulty ring of squirrel-cage	53.33
	TER [%]
4 analyzed states of three-phase induction motor	76.65

Table 4. Results of recognition of acoustic signal of three phase induction motor using SMOFS-20-EXPANDED and NBC.

State of three-phase induction motor	$CF = 0.64$
	ER [%]
Healthy three-phase induction motor	93.33
Three-phase induction motor with one faulty rotor bar	100
Three-phase induction motor with two faulty rotor bars	100
Three-phase induction motor with faulty ring of squirrel-cage	86.66
	TER [%]
4 analyzed states of three-phase induction motor	94.99

Table 5. Results of recognition of acoustic signal of three phase induction motor using SMOFS-20-EXPANDED and CT.

State of three-phase induction motor	$CF = 0.64$
	ER [%]
Healthy three-phase induction motor	73.33
Three-phase induction motor with one faulty rotor bar	100
Three-phase induction motor with two faulty rotor bars	53.33
Three-phase induction motor with faulty ring of squirrel-cage	80
	TER [%]
4 analyzed states of three-phase induction motor	76.65

ER was in the range of 86.66–100% for $CF = 0.64$ (Table 4). TER was equal 94.99% for SMOFS-20-EXPANDED and Naive Bayes classifier.

ER was in the range of 73.33–100% for $CF = 0.64$ (Table 5). TER was equal 76.65% for SMOFS-20-EXPANDED and classification tree.

The best results were obtained for $CF = 0.64$, SMOFS-20-EXPANDED and Naive Bayes classifier (Table 4).

4. Conclusions

The article presented a fault diagnostics system of three-phase induction motors. The presented system was based on acoustic signals of three-phase induction motors.

In this article the feature extraction method SMOFS-20-EXPANDED was described. The proposed method was used to diagnose incipient states of three-phase induction motors such as: healthy motor, motor with one faulty rotor bar, motor with two faulty rotor bars, motor with faulty ring of squirrel-cage. The classification step was performed using 3 classifiers: Linear Discriminant Analysis, Naive Bayes Classifier, Classification Tree. The best results were obtained for Naive Bayes classifier (Table 4). ER was in the range of 86.66–100% and TER was equal 94.99%.

The presented approach using acoustic signals is non-invasive and inexpensive. This approach can be used to diagnose three-phase induction motors with the same sizes and operational parameters. The presented approach can also find similar application for fault diagnostics of other types of electric motors and large-sized rotating machines (GLOWACZ, KOZIK, 2012; KUPIEC, PRZYBOROWSKI, 2015; SMOLNICKI *et al.*, 2010). In the future, acoustic, electric, and thermal signals should be used together to improve fault diagnostics of electric motors.

Acknowledgment

The research has been supported by AGH University of Science and Technology, grant nr 11.11.120.612.

References

1. ATTOUI I., OMEIRI A. (2015), *Fault Diagnosis of an Induction Generator in a Wind Energy Conversion System Using Signal Processing Techniques*, Electric Power Components and Systems, **43**, 20, 2262–2275.
2. BEDKOWSKI B., BARANSKI M. (2014), *Electrical machine with permanent magnets as a vibration sensor – a test stand model*, International Conference on Electrical Machines (ICEM), 1590–1593.
3. DUDEK-DYDUCH E., TADEUSIEWICZ R., HORZYK A. (2009), *Neural network adaptation process effectiveness dependent of constant training data availability*, Neurocomputing, **72**, 13–15, 3138–3149.
4. DUSPARA M., SABO K., STOIC A. (2014), *Acoustic emission as tool wear monitoring*, Tehnicki Vjesnik-Technical Gazette, **21**, 5, 1097–1101.
5. FIGLUS T., LISCAK S., WILK A., AAZARZ B. (2014), *Condition monitoring of engine timing system by using wavelet packet decomposition of a acoustic signal*, Journal of Mechanical Science and Technology, **28**, 5, 1663–1671.
6. GLOWACZ A. (2015), *Recognition of Acoustic Signals of Synchronous Motors with the Use of MoFS and Selected Classifiers*, Measurement Science Review, **15**, 4, 167–175.
7. GLOWACZ A., GLOWACZ A., GLOWACZ Z. (2012), *Diagnostics of Direct Current generator based on analysis of monochrome infrared images with the application of cross-sectional image and nearest neighbor classifier with Euclidean distance*, Przegląd Elektrotechniczny, **88**, 6, 154–157.
8. GLOWACZ W., GLOWACZ Z. (2015), *Diagnostics of separately excited DC motor based on analysis and recognition of signals using FFT and Bayes classifier*, Archives of Electrical Engineering, **64**, 1, 29–35.
9. GLOWACZ Z., GLOWACZ A. (2007), *Simulation language for analysis of discrete-continuous electrical systems (SESL2)*, 26th IASTED International Conference on Modelling, Identification and Control Location: Innsbruck, Austria, 94–99.
10. GLOWACZ Z., KOZIK J. (2012), *Feature selection of the armature windings short circuit fault in synchronous motor using genetic algorithm and the Mahalanobis distance*, Przegląd Elektrotechniczny, **88**, 2, 204–207.
11. GLOWACZ Z., ZDROJEWSKI A. (2009), *Diagnostics of commutator DC motor using spectral analysis method*, Przegląd Elektrotechniczny, **85**, 1, 147–150.
12. GONZALEZ-CORDOBA JL., GRANADOS-LIEBERMAN D., OSORNIO-RIOS RA., ROMERO-TRONCOSO RJ., DE SANTIAGO-PEREZ JJ., VALTIERRA-RODRIGUEZ M. (2016), *Methodology for Overheating Identification on Induction Motors under Voltage Unbalance Conditions*

- in Industrial Processes*, Journal of Scientific & Industrial Research, **75**, 2, 100–107.
13. GORNY Z., KLUSKA-NAWARECKA S., WILK-KOŁODZIEJCZYK D., REGULSKI K. (2015), *Methodology for the construction of a rule-based knowledge base enabling the selection of appropriate bronze heat treatment parameters using rough sets*, Archives of Metallurgy and Materials, **60**, 1, 309–312.
 14. HACHAJ T. (2012), *Pattern Classification Methods for Analysis and Visualization of Brain Perfusion CT Maps*, Computational Intelligence Paradigms in Advanced Pattern Classification, Book Series: Studies in Computational Intelligence, **386**, 145–170.
 15. HACHAJ T., OGIELA MR., KOPTYRA K. (2015), *Application of Assistive Computer Vision Methods to Oyama Karate Techniques Recognition*, Symmetry-Basel, **7**, 4, 1670–1698.
 16. HEMMATI F., ALQARADAWI M., GADALA MS. (2016), *Rolling element bearing fault diagnostics using acoustic emission technique and advanced signal processing*, Proceedings of the Institution of Mechanical Engineers Part J-Journal of Engineering Tribology, **230**, 1, 64–77.
 17. HWANG DH., YOUN YW., SUN JH., CHOI KH., LEE JH., KIM YH. (2015), *Support Vector Machine Based Bearing Fault Diagnosis for Induction Motors Using Vibration Signals*, Journal of Electrical Engineering & Technology, **10**, 4, 1558–1565.
 18. IRFAN M., SAAD N., IBRAHIM R., ASIRVADAM VS. (2015), *An on-line condition monitoring system for induction motors via instantaneous power analysis*, Journal of Mechanical Science and Technology, **29**, 4, 1483–1492.
 19. IZADBAKSH M., REZVANI A., GANDOMKAR M. (2015), *Dynamic response improvement of hybrid system by implementing ANN-GA for fast variation of photovoltaic irradiation and FLC for wind turbine*, Archives of Electrical Engineering, **64**, 2, 291–314.
 20. JAWOREK-KORJAKOWSKA J., KLECZEK P. (2016), *Automatic Classification of Specific Melanocytic Lesions Using Artificial Intelligence*, BioMed Research International, Article Number: 8934242.
 21. JENA DP., PANIGRAHI SN. (2015), *Automatic gear and bearing fault localization using vibration and acoustic signals*, Applied Acoustics, **98**, 20–33.
 22. JIANG Y., LI ZX., ZHANG C., HU C., PENG Z. (2016), *On the bi-dimensional variational decomposition applied to nonstationary vibration signals for rolling bearing crack detection in coal cutters*, Measurement Science and Technology, **27**, 6, Article Number: 065103.
 23. JOZWIK J. (2016), *Identification and monitoring of noise sources of CNC machine tools by acoustic Holography methods*, Advances in Science and Technology-Research Journal, **10**, 30, 127–137.
 24. JUN S., KOCHAN O. (2014), *Investigations of Thermocouple Drift Irregularity Impact on Error of their Inhomogeneity Correction*, Measurement Science Review, **14**, 1, 29–34.
 25. JUN S., KOCHAN O., KOCHAN V., WANG CZ. (2016), *Development and Investigation of the Method for Compensating Thermoelectric Inhomogeneity Error*, International Journal of Thermophysics, **37**, 1. <http://dx.doi.org/10.1007/s10765-015-2025-x>.
 26. KALAFAT S., SAUSE MGR. (2015), *Acoustic emission source localization by artificial neural networks*, Structural Health Monitoring-An International Journal, **14**, 6, 633–647.
 27. KANG TJ., KIM J., BIN LEE S., YUNG C. (2015), *Experimental Evaluation of Low-Voltage Offline Testing for Induction Motor Rotor Fault Diagnostics*, IEEE Transactions on Industry Applications, **51**, 2, 1375–1384.
 28. KANTOCH E., AUGUSTYNIAK P., MARKIEWICZ M., PRUSAK D. (2014), *Monitoring activities of daily living based on wearable wireless body sensor network*, 2014 36th Annual International Conference of the IEEE Engineering in Medicine and Biology Society (EMBC), Book Series: IEEE Engineering in Medicine and Biology Society Conference Proceedings, 586–589.
 29. KARANDIKAR J., MCLEAY T., TURNER S., SCHMITZ T. (2015), *Tool wear monitoring using naive Bayes classifiers*, International Journal of Advanced Manufacturing Technology, **77**, 9-12, 1613–1626.
 30. KLUSKA-NAWARECKA S., WILK-KOŁODZIEJCZYK D., DAJDA J., MACURA M., REGULSKI K. (2014), *Computer-Assisted Integration of Knowledge in the Context of Identification of the Causes of Defects in Castings*, Archives of Metallurgy and Materials, **59**, 2, 743–746.
 31. KOZIELSKI M., SIKORA M., WROBEL L. (2016), *Decision support and maintenance system for natural hazards, processes and equipment monitoring*, Eksploatacja i Niezawodność–Maintenance and Reliability, **18**, 2, 218–228. <http://dx.doi.org/10.17531/ein.2016.2.9>
 32. KROLCZYK G.M., KROLCZYK J.B., LEGUTKO S., HUNJET A. (2014), *Effect of the disc processing technology on the vibration level of the chipper during operations*, Tehnicki Vjesnik-Technical Gazette, **21**, 2, 447–450.
 33. KROLCZYK J.B., GAPINSKI B., KROLCZYK G.M., SAMARDZIC I., MARUDA R.W., SOUCEK K., LEGUTKO S., NIESLONY P., JAVADI Y., STAS L. (2016a), *Topographic inspection as a method of weld joint diagnostic*, Tehnicki Vjesnik-Technical Gazette, **23**, 1, 301–306.
 34. KROLCZYK G.M., KROLCZYK J.B., MARUDA R.W., LEGUTKO S., TOMASZEWSKI M. (2016b), *Metrological changes in surface morphology of high-strength steels in manufacturing processes*, Measurement, **88**, 176–185.
 35. KULKA Z. (2011), *Advances in Digitization of Microphones and Loudspeakers*, Archives of Acoustics, **36**, 2, 419–436.
 36. KUPIEC E., PRZYBOROWSKI W. (2015), *Magnetic equivalent circuit model for unipolar hybrid excitation synchronous machine*, Archives of Electrical Engineering, **64**, 1, 107–117.

37. LARA R., JIMENEZ-ROMERO R., PEREZ-HIDALGO F., REDEL-MACIAS MD. (2015), *Influence of constructive parameters and power signals on sound quality and airborne noise radiated by inverter-fed induction motors*, Measurement, **73**, 503–514.
38. LI ZX., JIANG Y., HU C., PENG Z. (2016), *Recent progress on decoupling diagnosis of hybrid failures in gear transmission systems using vibration sensor signal: A review*, Measurement, **90**, 4–19.
39. MA SH., CHEN XQ. (2015), *The Acoustic Emission Signal Recognition based on Wavelet Transform and RBF Neural Network*, International Journal of Grid and Distributed Computing, **8**, 2, 167–175.
40. MARZEC M., KOPROWSKI R., WROBEL Z. (2015), *Methods of face localization in thermograms*, Biocybernetics and Biomedical Engineering, **35**, 2, 138–146.
41. MICHALAK M., SIKORA M., SOBCZYK J. (2013), *Analysis of the longwall conveyor chain based on a harmonic analysis*, Eksploatacja i Niezawodność – Maintenance and Reliability, **15**, 4, 332–336.
42. MIKA D., JOZWIK J. (2016), *Normative measurements of noise at CNC machines work stations*, Advances in Science and Technology-Research Journal, **10**, 30, 138–143.
43. PANEK D., SKALSKI A., GAJDA J., TADEUSIEWICZ R. (2015), *Acoustic analysis assessment in speech pathology detection*, International Journal of Applied Mathematics and Computer Science, **25**, 3, 631–643.
44. PERUN G., STANIK Z. (2015), *Evaluation of state of rolling bearings mounted in vehicles with use of vibration signals*, Archives of Metallurgy and Materials, **60**, 3, 1679–1683.
45. PRIBIL J., PRIBILOVA A. (2014), *GMM-Based Evaluation of Emotional Style Transformation in Czech and Slovak*, Cognitive Computation, **6**, 4, 928–939.
46. ROJ J., CICHY A. (2015), *Method of Measurement of Capacitance and Dielectric Loss Factor Using Artificial Neural Networks*, Measurement Science Review, **15**, 3, 127–131.
47. SAPENA-BANO A., PINEDA-SANCHEZ M., PUCHE-PANADERO R., MARTINEZ-ROMAN J., MATIC D. (2015), *Fault Diagnosis of Rotating Electrical Machines in Transient Regime Using a Single Stator Current's FFT*, IEEE Transactions on Instrumentation and Measurement, **64**, 11, 3137–3146.
48. SHARMA A., PALIWAL K. (2015), *Linear discriminant analysis for the small sample size problem: an overview*, International Journal of Machine Learning and Cybernetics, **6**, 3, 443–454.
49. SMALCERZ A. (2013), *Aspects of Application of Industrial Robots in Metallurgical Processes*, Archives of Metallurgy and Materials, **58**, 1, 203–209.
50. SMOLNICKI T., HARNATKIEWICZ P., STANCO M. (2010), *Degradation of a geared bearing of a stacker*, Archives of Civil and Mechanical Engineering, **10**, 2, 131–139.
51. STEPIEN K. (2014), *Research on a surface texture analysis by digital signal processing methods*, Tehnicki Vjesnik-Technical Gazette, **21**, 3, 485–493.
52. STOLINSKI B., ZIOLKO B. (2015), *Detecting Recorded Speech for Polish Language*, Proceedings of the 2015 12th IEEE Africon International Conference – Green Innovation for African Renaissance (Africon), Book Series: Africon.
53. VALIS D., PIETRUCHA-URBANIK K. (2014), *Utilization of diffusion processes and fuzzy logic for vulnerability assessment*, Eksploatacja i Niezawodność – Maintenance and Reliability, **16**, 1, 48–55.
54. VAN HECKE B., YOON J., HE D. (2016), *Low speed bearing fault diagnosis using acoustic emission sensors*, Applied Acoustics, **105**, 35–44.
55. VETRICHELVAN G., SUNDARAM S., KUMARAN SS., VELMURUGAN P. (2015), *An investigation of tool wear using acoustic emission and genetic algorithm*, Journal of Vibration and Control, **21**, 15, 3061–3066.
56. WEGIEL T., SULOWICZ M., BORKOWSKI D. (2007), *A distributed system of signal acquisition for induction motors diagnostic*, 2007 IEEE International Symposium on Diagnostics for Electric Machines, Power Electronics & Drives, Cracow, Poland, 261–265.
57. WICKRAMARACHCHI DC., ROBERTSON BL., REALE M., PRICE CJ., BROWN J. (2016), *HHCART: An oblique decision tree*, Computational Statistics & Data Analysis, **96**, 12–23.
58. YAGAMI Y., ARAKI C., MIZUNO Y., NAKAMURA H. (2015), *Turn-to-Turn Insulation Failure Diagnosis of Stator Winding of Low Voltage Induction Motor with the Aid of Support Vector Machine*, IEEE Transactions on Dielectrics and Electrical Insulation, **22**, 6, 3099–3106.
59. YOON J., HE D. (2015), *Planetary gearbox fault diagnostic method using acoustic emission sensors*, IET Science Measurement & Technology, **9**, 8, 936–944.
60. ZHANG YG., YANG JY., WANG KC., WANG ZP. (2015), *Wind Power Prediction Considering Nonlinear Atmospheric Disturbances*, Energies, **8**, 1, 475–489.
61. ZHANG X., FENG NZ., WANG Y., SHEN Y. (2015), *Acoustic emission detection of rail defect based on wavelet transform and Shannon entropy*, Journal of Sound and Vibration, **339**, 419–432.